

Measurements of Inverse Bremsstrahlung Absorption and Non-Maxwellian Electron Velocity Distributions

J. M. Liu,¹ J. S. De Groot,¹ J. P. Matte,² T. W. Johnston,² and R. P. Drake³

¹*Plasma Research Group, Department of Applied Science, University of California, Davis, California 95616*

²*Institut National de la Recherche Scientifique-Energie et Matériaux, C.P. 1020, Varennes, Québec, Canada J3X 1S2*

³*Plasma Physics Research Institute, Lawrence Livermore National Laboratory, L-418,*

P.O. Box 808, Livermore, California 94551

(Received 15 December 1993)

Non-Maxwellian (flattopped) electron velocity distributions resulting from inverse bremsstrahlung of intense microwaves are measured directly for the first time in experiments performed on the UCD AURORA II device. The experiments are performed in the afterglow of a pulsed discharge plasma that is moderately collisional and sufficiently ionized ($\sim 1\%$) that Coulomb collisions are dominant. Langmuir probe measurements indicate that the isotropic component of the electron velocity distribution is non-Maxwellian in very good agreement with electron kinetic (Fokker-Planck) simulations.

PACS numbers: 52.50.Gj, 52.25.-b, 52.50.Jm, 52.65.+z

Systems of particles in equilibrium are well known to have Maxwellian particle velocity distributions. Plasmas are rarely in equilibrium, but nonetheless Coulomb collisions (and sometimes electrostatic fluctuations) are generally rapid enough that driven, steady-state plasmas most often exhibit Maxwellian or piecewise Maxwellian velocity distributions. Thus, any mechanism that systematically produces non-Maxwellian velocity distributions is of fundamental interest. Some time ago, Langdon [1] predicted that non-Maxwellian (flattopped) distributions would be produced in plasmas heated by inverse bremsstrahlung (collisional) absorption of sufficiently strong electromagnetic radiation. Although numerical simulations of laser-target interaction have supported this prediction [2,3], the present work is its first experimental verification. This is particularly significant since anomalously Maxwellian distributions have a long history in plasma physics, beginning with those of Langmuir's paradox [4].

This subject also has considerable practical import for x-ray lasers [5], x-ray sources [6], and laser fusion. Inverse bremsstrahlung absorption is dominant in the warm, long-scale-length plasmas produced when lasers irradiate high gain pellets [7]. In some pellet designs, the average ionic charge Z and the laser intensity are large enough that the distribution function is predicted to be non-Maxwellian. This occurs when collisional heating that preferentially heats low energy electrons is in competition with electron-electron collisions that tend to maintain the Maxwellian. This has important consequences: reduction of the absorption rate [1], the electron heat flux [8], and the threshold of the ion acoustic drift instability [9], and modification of the continuum x-ray emission rates [10,11] and the excitation and ionization rates [12]. Non-Maxwellian distributions are predicted when the parameter $\alpha \sim 1$ (here, $\alpha = Zv_{os}^2/v_e^2$, where v_{os} is the oscillating velocity of the electron in the electric field, E_0 , of the electromagnetic wave, $v_{os} = eE_0/m_e\omega_0$, m_e is the electron mass, ω_0 is the frequency of the electromagnetic wave, and v_e is the electron thermal speed, $v_e = \sqrt{T_e/m_e}$). In this case, the isotropic component of the electron velocity distribution, f_{e0} , is not Maxwellian but flattopped, i.e., $f_{e0} \sim \exp[-(v/v_m)^m]$, with the index $m > 2$, $v_m^2 = v_e^2 3\Gamma(3/m)/\Gamma(5/m)$, where $\Gamma(x)$ is the gamma function. For non-Maxwellian distributions, T_e is the kinetic temperature, i.e., $\frac{2}{3}$ of the average kinetic energy.

In this paper, we present the first direct measurements of flattopped electron velocity distributions due to inverse bremsstrahlung heating by intense electromagnetic waves. Langmuir probes are used to measure the spatial and temporal evolution of the isotropic component of the electron velocity distribution function. Our experimental results show that the distribution is indeed flattopped when the plasma is heated by intense microwaves. The measured results are in very good agreement with Fokker-Planck simulations.

The experiments are performed in the UCD AURORA II device, an improved version of the UCD AURORA device [13]. The improvements are the following: higher plasma fractional ionization, higher microwave power, a variable density gradient, and a greatly improved data acquisition and analysis system. The plasma is created by a pulsed discharge in low pressure argon ($P \sim 0.3$ mTorr, neutral density $n_{\text{argon}} \sim 10^{13} \text{ cm}^{-3}$). The argon pressure is low enough that the high power microwaves do not significantly increase the fractional ionization. Permanent magnets are arranged on the surface of the cylindrical vacuum chamber to increase the fractional ionization ($\sim 1\%$) and to produce an axial plasma density gradient. The axial density gradient is controlled by biasing anodes that are placed along the discharge length. At the time of the heating experiment, the plasma density increases approximately linearly with the axial coordinate z , and the critical density is reached at $z = 150$ cm. A microwave reflector (at $z = 70$ cm, optical transparency

$\sim 97\%$) divides the 200 cm long plasma axially into a short microwave absorption region ($0 \leq z \leq 70$ cm) and a longer transport region ($70 \leq z \leq 200$ cm). The microwaves are therefore excluded from the critical density region by the reflector so collective phenomena that would otherwise occur near the critical density do not affect the results discussed here.

The microwave heating experiments are performed in the afterglow plasma. The electron density is monitored and the microwave pulse is initiated when the density decays to a preset value (typically $n_e \sim n_{\max}/2$). By then, the afterglow temperature has decreased to $T_{e0} = 0.4$ eV, so that electron-charged particle collisions are strongly dominant over electron-neutral collisions, and the electron distribution is Maxwellian. A short microwave pulse (vacuum wavelength $\lambda_0 = 10$ cm, frequency $f_0 = 3.0$ GHz, critical density $n_{cr} = 1.1 \times 10^{11}$ cm $^{-3}$, and pulse width ~ 2 μ s) heats the plasma in the absorption region ($n_e/n_{cr} \lesssim 0.5$). The microwaves are transported in a rectangular waveguide (TE $_{10}$ mode) and converted to the circular TM $_{01}$ mode. This mode is adiabatically transformed so that the plasma filled vacuum vessel (diameter of 26 cm) is the cylindrical waveguide. A microwave filter is placed at the entrance ($z = 0$) to the absorption region so that only the TM $_{01}$ mode interacts with the plasma. The microwave power can be varied up to 90 kW, thus giving $\alpha_0 = Zv_{os}^2/v_{e0}^2 \lesssim 2$, even though $Z = 1$ in our plasma. The microwaves form a standing wave pattern in the absorption region since only a small ($\lesssim 5\%$) fraction of the incident microwaves are absorbed. Ion acoustic turbulence is not significant in our present experiments because the decay time of the electron heat flux is shorter than the growth time of the ion acoustic drift instability. Several cylindrical Langmuir probes are placed with their axes perpendicular to the plasma axis to measure the isotropic component of the electron velocity distribution function. The data acquisition system is based on LabVIEW 2 [14]. The repetition rate is 60 s $^{-1}$, thus allowing a large amount of data to be obtained in a short time.

Typical probe current versus probe voltage data are shown in Fig. 1. The isotropic component of the electron distribution function is proportional to the derivative of the probe current with respect to the probe voltage. The electron temperature T_e , density n_e , and distribution function index m are obtained by fitting the data by probe theory [15,16] that is modified to include flattopped velocity distributions. A typical fit to the data is shown in Fig. 1 along with a Maxwellian fit for comparison. The fit is very good over the range of the data or up to energies of about 3 times the electron temperature (about 90% of the electrons). The ion current contribution to the probe signal is negligible over the data range shown, but it prevents taking data at lower voltages, i.e., $V_{\text{probe}} \lesssim 2.2$ V (or higher electron energies). Each experimental data point is averaged over 128 shots to reduce the random noise. The large signal to noise ratio (> 100) results in quite good measurement accuracy:

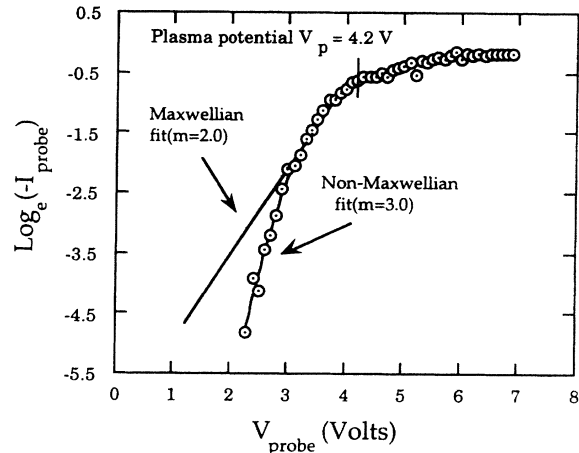


FIG. 1. Typical probe data (probe current I_{probe} as a function of probe voltage V_{probe}) taken right after the end of the microwave pulse ($t = 0$) with microwave power $P = 15$ kW. Each point is the average of 128 samples. The probe is located in the absorption region at a distance of 55 cm from the plasma boundary at $z = 0$. A flattopped distribution fits the data very well and a Maxwellian distribution does not agree with the data. The resulting parameters are $T_e = 0.69$ eV ($\frac{2}{3}$ of the average kinetic energy) and the plasma density $n_e = 4.0 \times 10^{10}$ cm $^{-3}$.

$\pm 7\%$ for T_e and $\pm 3\%$ for m . Such distribution functions that clearly differ from a Maxwellian were seen in previous calculations of inverse bremsstrahlung heating [1-3,10,12]. Moreover, we have found that, in the heating region, the dependence of the index m on the quiver energy and the temperature matches earlier calculations fairly well [10,12].

The plasma behavior was modeled with our planar one-dimensional electron kinetic code FPI (Fokker-Planck International) [2,10,13], since the ratio of the electron mean free path to the temperature gradient scale length was as high as 1/2, while the limit of validity for classical Spitzer-Härm heat transport is less than 1/100. The code includes the following: transport (for each energy group), a self-consistent electric field to ensure quasineutrality, electron-electron and electron-ion collisions in the Fokker-Planck approximation, and a kinetic heating operator [1] that is used to calculate the collisional absorption of the microwaves. The electromagnetic wave equation for the TM $_{01}$ mode was solved (using the measured plasma density profile, but neglecting the weak absorption) to find the quiver energy of electrons in the absorption region. This quiver energy was volume averaged over the radial coordinate to produce a one-dimensional axial profile of the quiver energy which is used to evaluate the heating operator. It was not necessary to correct for finite v_{os} in the heating operator [17] since the parameter α was always below 3. Electron-neutral collisions were neglected, and so was hydrodynamics because the hydrodynamic time scale is much longer than either the

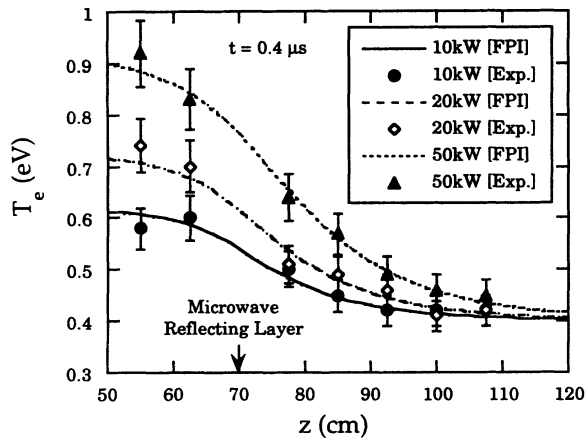


FIG. 2. Electron temperature T_e as a function of axial position with microwave power as a parameter (the origin, $z=0$, is at the plasma boundary). These measurements (symbols) and FPI kinetic code simulations (lines) were taken $0.4 \mu\text{s}$ after the end of the $2 \mu\text{s}$ microwave pulse.

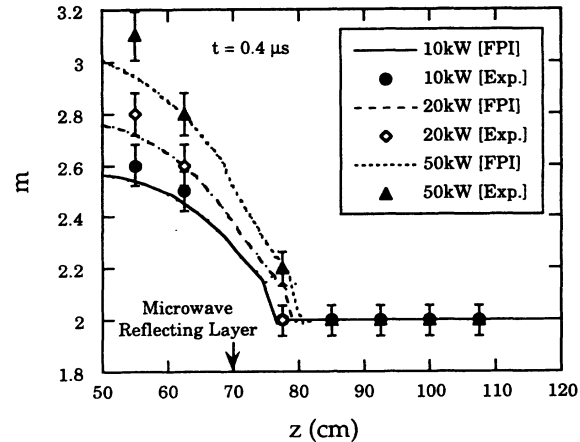


FIG. 3. Distribution function index m as a function of axial position with microwave power as a parameter (the origin, $z=0$, is at the plasma boundary). These measurements (symbols) and FPI kinetic code simulations (lines) were taken $0.4 \mu\text{s}$ after the end of the $2 \mu\text{s}$ microwave pulse.

heating pulse or the decay time of the heat flux. In the present calculations, the angular dependence of the electron velocity distribution function was expanded to third order in Legendre polynomials. While the temperature is a normal output of the code, least-squares fitting to the isotropic component of the electron velocity distribution of the form $\exp[-(v/v_m)^m]$ was used to extract the local value of the index m for comparison with the measured results.

The measured spatial profiles of the electron temperature (symbols, Fig. 2) and distribution function index m , (symbols, Fig. 3) agree very well with the Fokker-Planck simulations (lines). The agreement is as good for the three microwave powers shown. There are no adjustable parameters in comparing the simulations with the measurements. All input parameters to the code are measured (incident microwave power, microwave pulse width, and unperturbed electron density and temperature profiles) or calculated from the measurements (quiver energy profile which was calculated from the measured density profile).

The very good agreement shown in Figs. 2 and 3 indicates that FPI models both inverse bremsstrahlung absorption *and* electron heat transport very well. Since the microwave pulse is short enough that most heated electrons remain in the absorption region during the pulse, very steep temperature gradients are obtained at high microwave powers, i.e., at microwave power $P=50 \text{ kW}$, the electron mean free path $\lambda_{ei} \sim \frac{1}{2} L_T$, where $L_T = [(dT_e/dz)/T_e]^{-1}$ is the temperature gradient scale length. A heat flux as high as $q \approx 0.3n_e v_e T_e$ was seen in the FPI simulations, due to the extremely steep temperature gradients. These steep temperature gradients and resultant large heat fluxes can also occur in laser driven pellets,

especially where a short pulse of very high power laser light heats a plasma. Note that the heated electron temperature (Fig. 2) extends farther into the transport region than the non-Maxwellian distributions (index $m > 2$, Fig. 3). This is because the index m is characteristic of the slower electrons with shorter mean free paths, whereas heat transport is dominated by faster electrons with longer mean free paths [2,3]. Although only slower electrons are measured by the probes, the good agreement for heat transport is an indirect proof that the FPI code correctly models the faster electrons as well.

In summary, we have obtained the first experimental confirmation of the predicted production of non-Maxwellian electron velocity distributions in plasmas that are heated by inverse bremsstrahlung absorption of intense electromagnetic waves. These results show that strongly driven plasmas can be successfully modeled by Fokker-Planck kinetic codes, in regimes where classical collisional physics is dominant, and turbulence has not developed significantly. This lends confidence to the use of such simulations to evaluate the consequences of heating plasmas by high power lasers for laser fusion and other applications.

The authors gratefully acknowledge fruitful discussions with W. L. Kruer, J. H. Rogers, and K. G. Estabrook. We would like to thank T. Hillyer, H. Bandeh, and A. Froeschner for their technical support. This work was sponsored by the Plasma Physics Research Institute and the Lawrence Livermore National Laboratory and was partially performed under the auspices of the U.S. Department of Energy by the Lawrence Livermore National Laboratory under Contract No. W-7405-Eng-48. J. P. Matte and T. W. Johnston were supported by le Ministère de l'Éducation du Québec and by the Natural

Science and Engineering Research Council of Canada.

-
- [1] A. Brue Langdon, *Phys. Rev. Lett.* **44**, 575 (1980).
- [2] J. P. Matte, T. W. Johnston, J. Delettrez, and R. L. McCrory, *Phys. Rev. Lett.* **53**, 1461 (1984); J. P. Matte and J. Virmont, *ibid.* **49**, 1936 (1982).
- [3] J. R. Albritton, *Phys. Rev. Lett.* **50**, 2078 (1983).
- [4] I. Langmuir, *Phys. Rev.* **26**, 585 (1925).
- [5] M. D. Rosen, *Phys. Fluids B* **2**, 1461 (1990).
- [6] R. Kodama *et al.*, *J. Appl. Phys.* **59**, 3050 (1986).
- [7] W. L. Kruer, *Comm. Plasma Phys.* **5**, 69 (1979).
- [8] P. Mora and H. Yahi, *Phys. Rev. A* **26**, 2259 (1982).
- [9] J. S. De Groot, K. G. Estabrook, W. L. Kruer, R. P. Drake, K. Mizuno, and S. M. Cameron, *Laser Interact. Relat. Plasma Phenom.* **10**, 197 (1992).
- [10] J. P. Matte, M. Lamoureux, C. Moller, R. Y. Yin, J. Delettrez, J. Virmont, and T. W. Johnston, *Plasma Phys. Controlled Fusion* **30**, 1665 (1988).
- [11] D. L. Matthews, R. L. Kauffman, J. D. Kilkenny, and R. W. Lee, *Appl. Phys. Lett.* **44**, 586 (1984).
- [12] P. Alaterre, J. P. Matte, and M. Lamoureux, *Phys. Rev. A* **34**, 1578 (1986).
- [13] J. H. Rogers, J. S. De Groot, Z. Abou-Assaleh, J. P. Matte, T. W. Johnston, and M. D. Rosen, *Phys. Fluids B* **1**, 741 (1989).
- [14] LabVIEW, National Instruments (6504 Bridge Point Parkway, Austin, TX 78730).
- [15] J. D. Shift and M. J. R. Schwar, *Electrical Probes for Plasma Diagnostics* (American Elsevier, New York, 1969).
- [16] J. H. Rogers, J. S. De Groot, and D. Q. Hwang, *Rev. Sci. Instrum.* **63**, 31 (1992).
- [17] L. Schlessinger and J. Wright, *Phys. Rev. A* **20**, 1934 (1979).